Miniaturization of Dual Shaped Monopole Antenna for UWB Application

Ranjeet Kumar, Rashmi Sinha, Arvind Choubey, Santosh Kumar Mahto, Pravesh Pal, and Praveen Kumar

Abstract With a recent development and phenomenal activity in the area of microwave, there is need to maintain quality of service and high data rate. Therefore, requirement to design an antenna which provide these facilities. This paper presents a double regular hexagonal radiating patch, defected ground, and small circular slot etched out from the middle part of radiating patch. It demonstrated the Ultra-Wide band (UWB) operation, which works efficiently in entire band from 2.52 to 12.91 GHz. The overall dimension of proposed antenna is 31 $\times$ 51.5 mm^2 Simulated in HFSS and has almost stable radiation pattern of E- and H-plane, positive gain of 6 dBi, and 134% of bandwidth in the entire band. This microstrip antenna is simulated and fabricated to verify its result, the equivalent circuit model is also constructed to verify simulate a measured result, which works efficiently in S, C, and X band applications.

Keywords Antenna theory · Bandwidth · Microstrip antenna

R. Kumar (✉) · R. Sinha · P. Pal · P. Kumar
Department of Electronics and Communication Engineering, National Institute of Technology, Jamshedpur, India
e-mail: ranjeet2k4kumar@gmail.com

R. Sinha
e-mail: rsinha.ece@nitjsr.ac.in

P. Pal
e-mail: praveshpal9@gmail.com

P. Kumar
e-mail: 2018rsec005@nitjsr.ac.in

A. Choubey
Indian Institute of Information Technology, Bhagalpur, India
e-mail: achoubey.ece@nitjsr.ac.in

S. K. Mahto
Department of Electronics & Communication Engineering, Indian Institute of Information Technology, Ranchi, India
e-mail: skumar@iiitranchi.ac.in

S. Dhar et al. (eds.), *Advances in Communication, Devices and Networking*, Lecture Notes in Electrical Engineering 902, https://doi.org/10.1007/978-981-19-2004-2_25

1 Introduction

Recently development in the field of wireless communication system, has led to demand of UWB antenna, which gives wide bandwidth, low transmission rate, less distortion, high gain and most importantly very less probability to intercept. Antenna researcher community face the problem and designed the miniaturized antenna to fulfill the requirement of UWB. The microstrip planar antenna is chosen because of its attractive feature of monitorization, low profile, low manufacturing cost and appropriate for production [1]. There are different shaped of UWB antenna has been demonstrated in [2–15]. A hexagonal antenna shaped with partial ground plane [2], L-shaped slot-based patch antenna for bandwidth enhancement [3], U-shaped aperture dual band UWB antenna [4], low profile band rejected radiating patch antenna [5], to prediction of notch frequency and T-shaped slot in partial ground [6, 7], a miniaturized antenna with band-notch characteristics, multi resonator, triangular-hexagonal based antenna for UWB antenna has been presented [8–11] to highlight the recently published works in the field of antenna.

This works has two regulars hexagonal shaped patch placed at 30° about its center and has a small circular slot at the middle of proposed antenna. It is designed on FR4 substrate of compact size 31 × 51.5 mm^2. This proposed antenna presented here has compact size, easy to fabricate, wide bandwidth, stable radiation pattern, and positive gain. The bandwidth of antenna may be enhanced by inserting the circular slot at it center.

2 Antenna Design and Implementation

The proposed microstrip feed hexagonal printed antenna and its evolution step are show in Fig. 1. A double regular hexagonal radiating patch, defected ground, and small circular slot etched out from the middle part of radiating patch. In first step, a regular hexagonal shape (ANT1) of radius R is taken as depicted in Fig. 1a. A similar type regular hexagonal shape is placed at 30° to get ANT2 as shown in Fig. 1b. And finally, small circular slot is inserted on the center of radius 'r' to obtained ANT3 as portrayed in Fig. 1c. This antenna structure is designed on FR4 epoxy dielectric material constant of (ε) = 4.4, height (h) = 1.6 mm, and loss tangent (δ) = 0.02. The width of defected ground plane (wg) = 13.5 mm, radius of hexagonal patch (R) = 13 mm, and circular slot (r) = 2 mm is the optimized parameter of proposed antenna. Simulated and fabricated proposed antenna captured in Fig. 2a, b.

The resonant frequencies of regular Hexagonal Patch Antenna (HPA) are calculated by Eq. (1) [11].

$$f_0 = \frac{T_{mn} C}{5.714 R_e \sqrt{\varepsilon_{r\text{eff}}}} \tag{1}$$

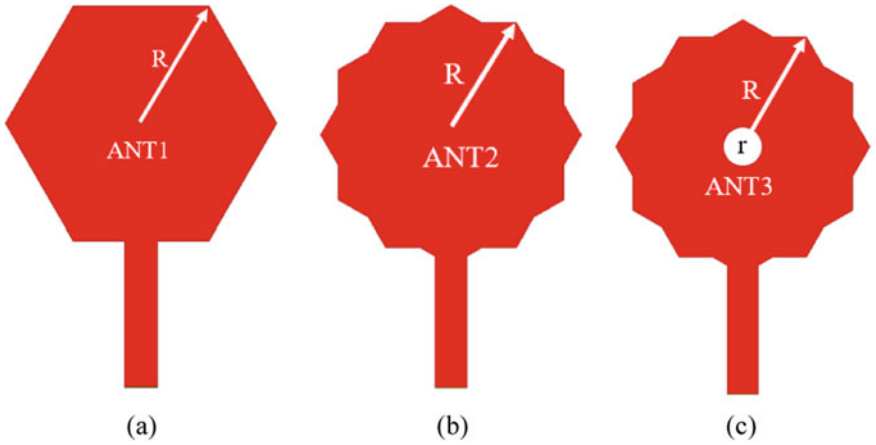

Fig. 1 Deriving stage of dual hexagonal shaped antenna

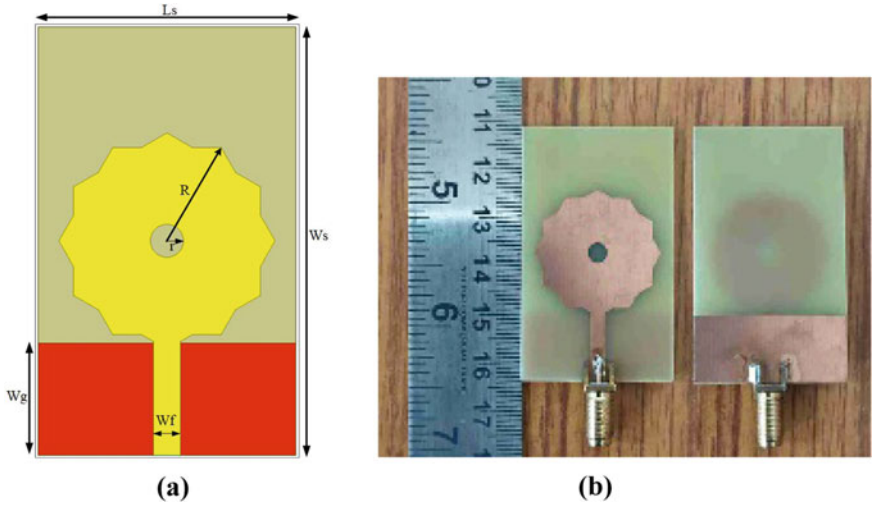

Fig. 2 **a** Simulated and **b** prototype antenna

where C = speed of electromagnetic wave in free space, $\varepsilon_{\text{reff}}$ = effective dielectric material constant, the operative radius (R_e) of patch antenna is calculated through Eq. (2) [11].

$$R_e = R_c.\sqrt{\left(1 + \frac{2.h}{R_c.\pi.\varepsilon_r}\left[\ln\left(\frac{\pi.R_c}{2.h}\right) + 1.7726\right]\right)} \tag{2}$$

where R_c, h, ε_r is the radius of the circular geometry, thickness, and material dielectric constant, respectively. By equating the area of circular and hexagonal shape, the resonance frequency can be determined by Eq. (3) [11].

$$\pi.(R_e)^2 = (1.5).\sqrt{3}.(S_h)^2 \tag{3}$$

Effective dielectric material constant (ε_{reff}) is given by Eq. (4) [11]

$$\varepsilon_{reff} = \frac{1+\varepsilon_r}{2} \tag{4}$$

where S_h, ε_r are the side of hexagonal patch and relative dielectric constant.

3 Finite Element Method (FEM) Analysis

In this section, FEM is used to demonstrate the how and at what extend the potential is varied. Partial differential equation (PDE), in MATLAB toolbox, helps to analyze numerically. There are 223 elements, 55 edges, and 139 nodes available in this antenna. The elliptical, parabolic, hyperbolic form of generic mode and electric, magnetic form of electromagnetic mode are calculated through Eqs. (5–9) [12] and it is graphical representation is depicted in Fig. 3.

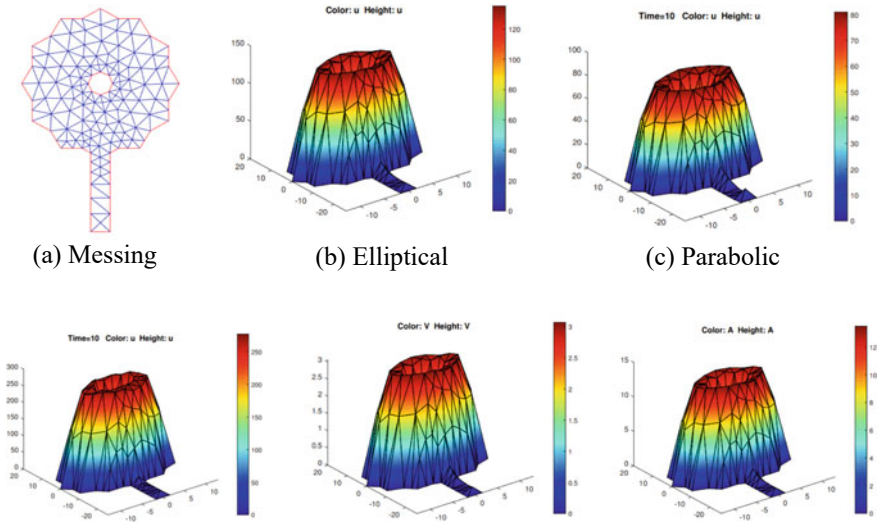

(a) Messing (b) Elliptical (c) Parabolic

(d) Hyperbolic (e) Electrostatics (f) Magnetostatics

Fig. 3 The variation of potential in different modes

$$-div(c * grad(U)) + a * U = f \tag{5}$$

$$d * U' - \text{div}(c * \text{grad}(U)) + a * U = f \tag{6}$$

$$d * U'' - \text{div}(c * \text{grad}(U)) + a * U = f \tag{7}$$

$$-\text{div}(\varepsilon * \text{grad}(U)) = \rho, \mathbf{E} = -\text{grad}(U) \tag{8}$$

$$-\text{div}\left(\frac{1}{\mu} * \text{grad}(\boldsymbol{A})\right) = \boldsymbol{J}, \boldsymbol{B} = -\text{curl}(A) \tag{9}$$

where $U =$ scalar potential, $f =$ source, $\mathbf{E} =$ electric field, $\mathbf{B} =$ magnetic field density, $\mathbf{A} =$ magnetic vector potential, $\rho =$ charge density, $\varepsilon =$ coefficient of dielectric, $\mu =$ magnetic permeability, and a, c, d are scalar constant.

4 Lumped Circuit Model Analysis

The return loss characteristic of radiating microstrip patch antenna is developed by help of transmission line model. Its result can be verified by lumped equivalent circuit model. This model can be constructed using basic elements of resistor (R), inductor (L), capacitor (C), and conductance (G). The microstrip feedline, resonating patch, and partial ground can be approximated as a series combination of surface resistance (R_s), and surface inductance (L_s) and is calculated by Eq. (10–11) [13–16]

$$R_s = \frac{1}{W_f \sigma_{\text{cond}}\, \delta} \tag{10}$$

$$L_s = \frac{1}{W_f \sigma_{\text{cond}}\, \delta\omega} \tag{11}$$

where $\delta = \sqrt{\frac{2}{\omega\sigma_{\text{cond}}\,\mu_0}}$ and

The conducting top and bottom layer are separated by FR-4 substrate. Electrically, this suggest a parallel combination of capacitor C and its value is calculated by Eq. (12) [13–16]. The conductance G, due to dielectric loss can be omitted for sake of simple analysis.

$$C = \varepsilon_{r\text{eff}} 2.85 \frac{1}{\ln\left\{1 + \frac{1}{2}\left(\frac{8h}{W_{\text{eff}}}\right)\left[\left(\left(\frac{8h}{W_{\text{eff}}}\right) + \sqrt{\left(\frac{8h}{W_{\text{eff}}}\right)^2 + \pi^2}\right)\right]\right\}} \tag{12}$$

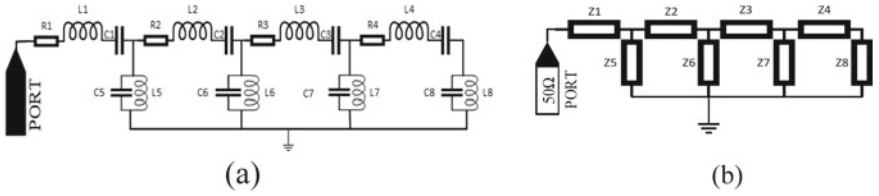

Fig. 4 **a** Equivalent circuit model antenna, **b** Reduced form

where

$$W_{\text{eff}} = W_f + \frac{t}{\pi} \ln \left\{ \frac{4e}{\sqrt{\left(\frac{t}{h}\right)^2 + \left[\frac{1}{\pi\left(\frac{W_f}{t} + 1.10\right)}\right]^2}} \right\}$$

where $t =$ conductor height, $\sigma_{\text{cond}} =$ surface conductivity, $\omega =$ angular frequency, $\delta =$ skin depth, $C =$ capacitance of capacitor, $W_{\text{eff}} =$ effective width, and $\varepsilon_{r\text{eff}} =$ effective material dialectic constant, $\mu_0 =$ permeability in the free space. All assumptions are considered and lumped equivalent circuit is drawn as Fig. 4.

The input impedance (Zin $= R + jX$) is numerically calculated from Fig. 4b.

$$Zi = Ri + j\omega Li + \frac{1}{j\omega Ci} = Ri + \frac{1 - \omega^2 CiLi}{j\omega Ci};$$

and

$$\text{Zn} = \frac{j\omega Ln \times \frac{1}{j\omega Cn}}{j\omega Ln + \frac{1}{j\omega Cn}} = \frac{j\omega Ln}{1 - \omega^2 CnLn}$$

where $i = 1, 2, 3, 4$, and $n = 5, 6, 7, 8$; By putting the value of i and n, Z1 to Z8 can be obtained such as $i = 1$ and $n = 5$ will give

$$Z1 = R1 + j\omega L1 + \frac{1}{j\omega C1} = R1 + \frac{1 - \omega^2 C1L1}{j\omega C1};$$

and

$$Z5 = \frac{j\omega L5 \times \frac{1}{j\omega C5}}{j\omega L5 + \frac{1}{j\omega C5}} = \frac{j\omega L5}{1 - \omega^2 C5L5}$$

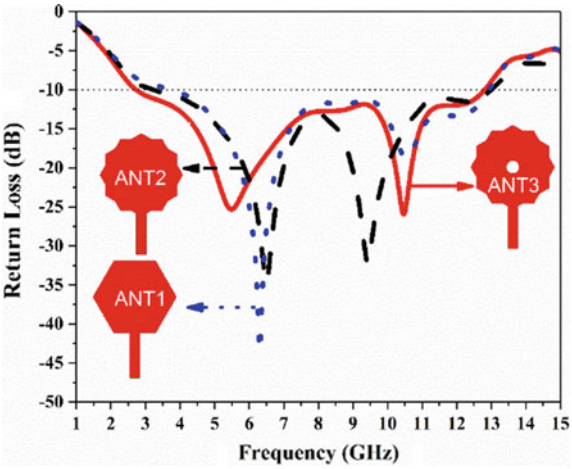

Fig. 5 Comparison of return loss of evolved antenna

Total input impedance (Zin) is calculated as,

$$Z_{in} = Z1 + \frac{Z5 \times \left[Z2 + \frac{Z6 \times \left\{ Z3 + \frac{(Z4+Z8)\times Z7}{Z4+Z8+Z7} \right\}}{Z6+Z3+\frac{(Z4+Z8)\times Z7}{Z4+Z8+Z7}} \right]}{Z5 + Z2 + \frac{Z6 \times \left\{ Z3 + \frac{(Z4+Z8)\times Z7}{Z4+Z8+Z7} \right\}}{Z6+Z3+\frac{(Z4+Z8)\times Z7}{Z4+Z8+Z7}}} \tag{13}$$

The reflection coefficient (Γ) is determined by Eq. (14) with help of Eq. (13). Voltage standing wave ratio (VSWR), and return loss (RL) is given by Eqs. (15–16), respectively.

$$\Gamma = \frac{Z_{\text{in}} - Z_0}{Z_{\text{in}} + Z_0} \tag{14}$$

$$\text{VSWR} = \frac{1 + |\Gamma|}{1 - |\Gamma|} \tag{15}$$

$$\text{Return loss} = 20 \log|\Gamma| \tag{16}$$

where Z_0 is the characteristic impedance (50Ω).

5 Result and Discussion

Performance parameters of the simulated and fabricated antenna are discussed in this section. The proposed antenna (ANT3) in Fig. 1c represents ultra-wide band characteristic as can be seen from Fig. 5. The observations and its values are enumerated in Table 1.

Figure 6, shows the scattering parameters of proposed antenna, which is obtained by simulation, measurement, and lumped circuit model. All outcomes are very close to each other. The simulated bandwidth of this antenna is of 13.09 GHz, ranging from 2.52–12.91 GHz. it can be seen from plot that there is little variation of return loss characteristic at lower and higher resonance frequency. The higher order modes are activated to enhance the wide bandwidth.

The E and H-plane, at its resonance frequencies of 5.4 and 10.4 GHz are depicted in Fig. 7 and can be seen from it that, simulated and measured radiation patterns are almost stable and has good co-polarization than cross-polarization.

The simulated and measured peak gain of the antenna is 6 dBi at 11.57 GHz depicted Fig. 8a. Average gain and radiation efficiency are 3.5 dBi and 87% in entire operating band as captured in Fig. 8b.

Table 1 Tabulated comparison between resonance frequencies

Antenna	1st resonance	2nd resonance	Bandwidth (GHz)
ANT1	6.5	9.4	3.17–13.00
ANT2	6.2	10.5	3.77–12.94
ANT3	5.4	10.4	2.52–12.91

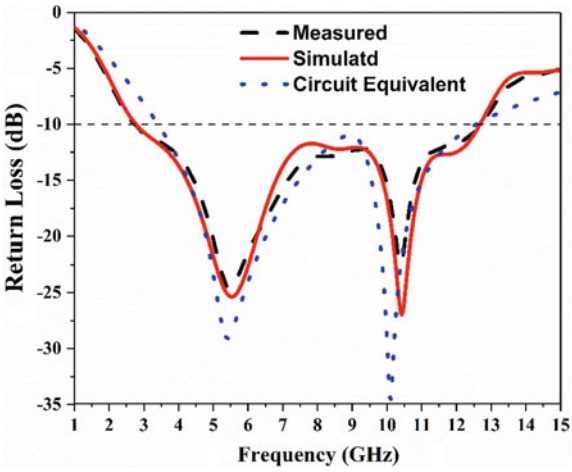

Fig. 6 Variation of return loss of the antenna

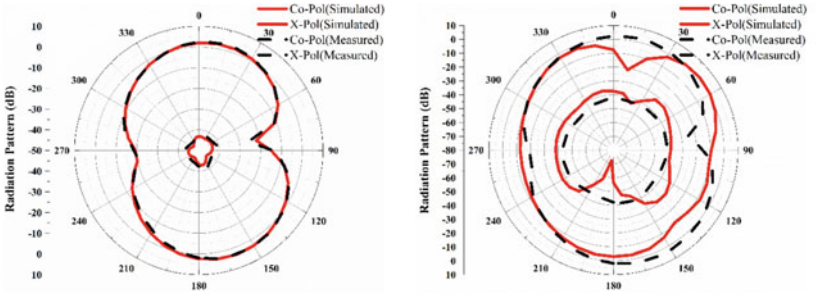

(a) 5.4 GHz (b) 10.4 GHz

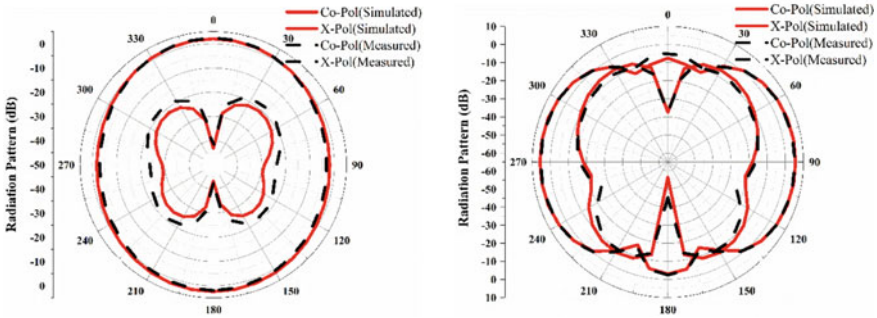

(c) 5.4 GHz (d) 10.4 GHz

Fig. 7 The simulated and measured **a**, **b** E-plane, and **c**, **d** H-plane

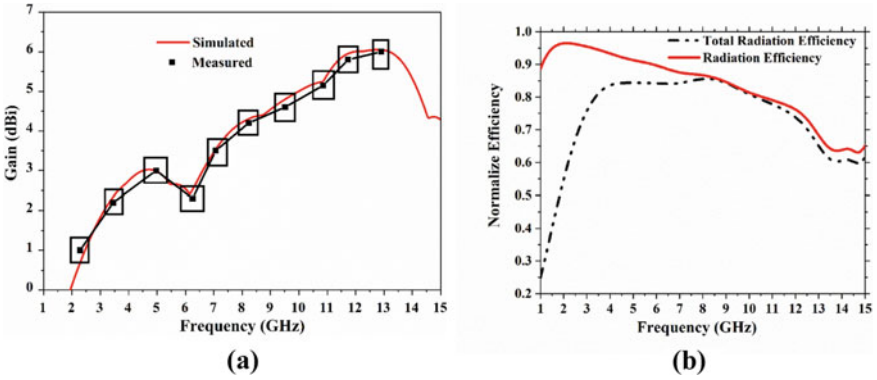

Fig. 8 **a** Peak gain, and **b** radiation efficiency versus frequency

6 Conclusion

This paper presents dual hexagonal shaped microstrip antenna with partial ground plane of $31 \times 51.5\ mm^2$, which exhibits an impedance bandwidth of 10.39 GHz, with VSWR less than 2. The proposed antenna confirms that it maintains the favorable conditions for UWB applications such as WLAN, WiMAX, 5G, S, C, and X band. There is a little discrepancy in simulated and measured results due to permissible fabrication error.

References

1. Yang HD (2005) Miniaturized printed wire antenna for wireless communications. IEEE Antennas Wirel Propag Lett 4:358–361
2. Pramudita AA, Kurniawan A, Suksmono AB (2008) Hexagonal monopole strip antenna with rectangular slot for 100–1000 MHz SFCW GPR applications. Int J Antennas Propag
3. Zaker R, Ghobadi C, Nourinia J (2009) Bandwidth enhancement of novel compact single and dual band-notched printed monopole antenna with a pair of L-shaped slots. IEEE Trans Antennas Propag 57(12):3978–3983
4. Zhou HJ, Sun BH, Liu QZ, Deng JY (2008) Implementation and investigation of U-shaped aperture UWB antenna with dual band-notched characteristics. Electron Lett 44(24):1387–1388
5. Jang JW, Hwang HY (2009) An improved band-rejection UWB antenna with resonant patches and a slot. IEEE Antennas Wirel Propag Lett 8:299–302
6. Dissanayake T, Esselle KP (2007) Prediction of the notch frequency of slot loaded printed UWB antennas. IEEE Trans Antennas Propag 55(11):3320–3325
7. Ojaroudi M, Ghobadi C, Nourinia J (2009) Small square monopole antenna with inverted T-shaped notch in the ground plane for UWB application. IEEE Antennas Wirel Propag Lett 8:728–731
8. Liu J, Gong S, Xu Y, Zhang X, Feng C, Qi N (2008) Compact printed ultra-wideband monopole antenna with dual band-notched characteristics. Electron Lett 44(12):710–711
9. Chang TN, Wu MC (2008) Band-notched design for UWB antennas. IEEE Antennas Wirel Propag Lett 7:636–640
10. Ma TG, Hua RC, Chou CF (2008) Design of a multiresonator loaded band-rejected ultrawideband planar monopole antenna with controllable notched bandwidth. IEEE Trans Antennas Propag 56(9):2875–2883
11. Darimireddy NK, Reddy RR, Prasad AM (2018) A miniaturized hexagonal-triangular fractal antenna for wide-band applications [antenna applications corner]. IEEE Antennas Propag Mag 60(2):104–110
12. Sadiku MN (2018) Computational electromagnetics with MATLAB. CRC Press
13. Bogatin E (1988) Design rules for microstrip capacitance. IEEE Trans Comp, Hybrids, Manuf Technol 11(3):253–259
14. Bahl I, Bhartia P, Stuchly S (1982) Design of microstrip antennas covered with a dielectric layer. IEEE Trans Antennas Propag 30(2):314–318
15. Garg R, Bhartia P, Bahl IJ, Ittipiboon A (2001) Microstrip antenna design handbook. Artech House
16. Balanis CA (2016) Antenna theory: analysis and design. Wiley